Spin- and valley-dependent commensurability oscillations and electric-field-induced quantum Hall plateaux in periodically modulated silicene

Kh. Shakouri, P. Vasilopoulos, V. Vargiamidis, G.-Q. Hai, and F. M. Peeters

Articles you may be interested in

Quantum spin/valley Hall effect and topological insulator phase transitions in silicene
Appl. Phys. Lett. **102**, 162412 (2013); 10.1063/1.4803084

Quantum spin Hall effect induced by electric field in silicene
Appl. Phys. Lett. **102**, 043113 (2013); 10.1063/1.4790147

Nuclear Spin Resonance Induced by Radio Frequency Electric Field
AIP Conf. Proc. **1199**, 461 (2010); 10.1063/1.3295506

Electrical polarization of nuclear spins in a breakdown regime of quantum Hall effect
Appl. Phys. Lett. **90**, 022102 (2007); 10.1063/1.2431453

Shubnikov–de Haas oscillations, peaks, and different temperature regimes of the diagonal conductivity in the integer quantum Hall conductor
Low Temp. Phys. **31**, 628 (2005); 10.1063/1.2001651

Spin- and valley-dependent commensurability oscillations and electric-field-induced quantum Hall plateaux in periodically modulated silicene

Kh. Shakouri,[1] P. Vasilopoulos,[2] V. Vargiamidis,[2] G.-Q. Hai,[3] and F. M. Peeters[1]

[1]*Departement Fysica, Universiteit Antwerpen, Groenenborgerlaan 171, B-2020 Antwerpen, Belgium*
[2]*Department of Physics, Concordia University, 7141 Sherbrooke Ouest Montréal, Québec H4B 1R6, Canada*
[3]*Instituto de Fisica de São Carlos, Universidade de São Paulo, São Carlos, SP 13560-970, Brazil*

We study the commensurability oscillations in silicene subject to a perpendicular electric field E_z, a weak magnetic field B, and a weak periodic potential $V = V_0 \cos(Cy)$, $C = 2\pi/a_0$ with a_0 its period. The field E_z and/or the modulation lift the spin degeneracy of the Landau levels and lead to spin and valley resolved Weiss oscillations. The spin resolution is maximal when the field E_z is replaced by a periodic one $E_z = E_0 \cos(Dy)$, $D = 2\pi/b_0$, while the valley one is maximal for $b_0 = a_0$. In certain ranges of B values, the current is fully spin or valley polarized. Additional quantum Hall conductivity plateaus arise due to spin and valley intra-Landau-level transitions. © 2014 AIP Publishing LLC.
[http://dx.doi.org/10.1063/1.4878509]

A monolayer honeycomb structure of silicon, called silicene, has been predicted to be stable[1] and several attempts have been made to synthesize it.[2] Silicene has Dirac cones similar to those of graphene but contrary to it, in which the spin-orbit interaction (SOI) is very weak, silicene has a strong SOI due to its low-buckled geometry and large atomic intrinsic SOI that leads to a gap of 1.55 meV.[3] This gap can be further controlled by an external electric field E_z and is facilitated by the buckled structure of silicene. This and its compatibility with silicon-based technology led already to many studies, reviewed in Ref. 4, such as the spin-Hall effect[3,5] and the capacitance of an electrically tunable silicene device.[6] Moreover, very recent theoretical studies predict the stability of silicene on nonmetallic surfaces such as graphene,[7] boron nitride or SiC,[9] and in graphene-silicene-graphene structures.[8]

Since the SOI can lead to spin-resolved transport, pertinent to quantum computing, it is worth studying it further in silicene and contrast the results with those for graphene in which the SOI is very weak. We explore the influence of SOI on the commensurability or Weiss oscillations[10] in silicene in the presence of the field E_z, of a perpendicular magnetic field $B||z$, and of a *weak periodic* potential $V(y) = V_0 \cos(Cy)$. These oscillations result from the fact that modulation-broadened Landau levels (LLs) have a bandwidth that oscillates with *weak B* and express the commensurability between the modulation period and the cyclotron diameter at the Fermi level. The study is an extension of that for a two-dimensional electron gas (2DEG)[11] and of that for graphene.[12,13] In addition, we consider a periodic field $E_z = E_0\cos(Dy)$. If one or two such modulations is present, the spin degeneracy is lifted and leads to spin-dependent commensurability oscillations when B is varied; the lifting is stronger for a periodic field E_z.

Unmodulated silicene. The one-electron Hamiltonian, near the K and K' valleys, in a magnetic field B, in the Landau gauge for the vector potential $\mathbf{A}$, is[3]

$$H = v_F(\pi_x \sigma_x - \tau\pi_y \sigma_y) - (\tau s_z \lambda_{so} - \ell E_z)\sigma_z, \qquad (1)$$

after shifting the wave vectors k_x and k_y by $eA_\mu/\hbar$, $\mu = x, y$, i.e., by setting $\mathbf{\Pi} = \mathbf{p} + e\mathbf{A}$, with $\mathbf{p}$ is the momentum operator and e is the electron charge. Here, v_F is the Fermi velocity, $\tau = +(-)$ is the K (K') valley index, σ_i ($i = x,y,z$) is the pseudospin Pauli matrices, 2ℓ is the vertical distance between the sublattices A and B, and E_z is an electric field normal to the silicene sheet, see Fig. 1. Further, λ_{so} is the SOI strength and $s_z = 1$ ($s_z = -1$) the up (down) electron spin. Inserting the factors τ and σ_i in Eq. (1) gives the Hamiltonian $H_\pm$ with the $+$ $(-)$ sign for the K (K') valley

$$H_\pm = \begin{bmatrix} \lambda_\pm(s_z) & v_F \pi_\pm \\ v_F \pi_\mp & -\lambda_\pm(s_z) \end{bmatrix}, \qquad (2)$$

where $\lambda_\pm(s_z) = \mp\lambda_{so}s_z + \ell E_z$ and $\pi_\pm = \pi_x \pm i\pi_y$. Using the gauge $A_x = -By$ and the ansatz $\Psi(x,y) = \exp(ik_x x)\psi(y)/\sqrt{L_x}$, with L_x the system's length in the x direction, leads to the eigenvalues

$$E_{n,s_z,p}^\pm = p\hbar\omega_c \left(n + [\bar{\lambda}_\pm(s_z)]^2\right)^{1/2}. \qquad (3)$$

Here, $p = +1(-1)$ labels the electron (hole) states, n ($n \geq 1$) is the LL index, $\bar{\lambda}_\pm = \lambda_\pm/\hbar\omega_c$, $\omega_c = \sqrt{2}v_F/l_B$, and $l_B = \sqrt{\hbar/eB}$. Note that the energy does not depend on k_x. Setting $\xi = y/l_B - l_B k_x$ the associated spatial eigenfunctions of an electron near the K point are

$$\psi_n^+(\xi) = \begin{pmatrix} \eta_1^+ \phi_n(\xi) \\ \eta_2^+ \phi_{n-1}(\xi) \end{pmatrix}, \qquad (4)$$
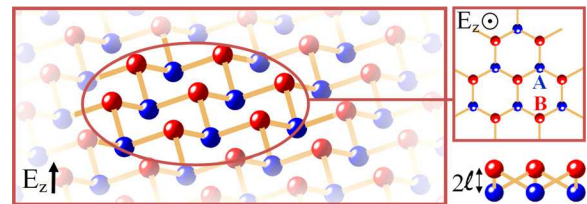

FIG. 1. Buckled honeycomb lattice of silicene. The two sublattices, formed by the blue and red atoms, are vertically separated by a distance 2ℓ.

with ϕ_n the normalized Harmonic oscillator function and

$$\eta_1^+ = \left[\frac{\lambda_+(s_z) + E_{n,s_z,p}^+}{2E_{n,s_z,p}^+}\right]^{1/2}, \quad \eta_2^+ = -p\left[\frac{E_{n,s_z,p}^+ - \lambda_+(s_z)}{2E_{n,s_z,p}^+}\right]^{1/2}. \tag{5}$$

For an electron near the K' valley, the results are similar. For $n = 0$, each valley involves only one solution with energy $E_{0,s_z}^\pm = \pm\hbar\omega_c\lambda_\pm(s_z)$ and eigenfunctions $\psi_0^+ = [\phi_0(\xi), 0]^T$ and $\psi_0^- = [0, \phi_0(\xi)]^T$. The electron energies at the K and K' valleys are related by $E_{n,\pm1,p}^+ = E_{n,\mp1,p}^-$ for $n \geq 1$, and $E_{0,\pm1}^+ = -E_{0,\mp1}^-$ for $n = 0$.

Modulated silicene. We now assess the influence of an external periodic potential and/or that of a modulated field E_z. As in the case of a 2DEG[10,11] or graphene,[12] the main effect of either modulation is to broaden the LLs into energy bands that oscillate with B and k_x. Each LL though splits into four branches, two for the valley and two for the spin degree of freedom due to the SOI.

(i) *Potential modulation.* We consider a periodic potential $V(y) = V_0\cos(Cy)$, $C = 2\pi/a_0$, with a_0 its period, added to H as $V(y)I$, with I is the identity matrix. For small V_0, we can use first-order perturbation theory to find the correction to the eigenvalues (3). For an electron near the K and K' valleys, the correction is

$$\Delta E_{n,s_z,p}^\pm(k_x) = V_0\cos(Cx_0)e^{-u/2}G_{n,s_z,p}^\pm, \tag{6}$$

$$G_{n,s_z,p}^+ = |\eta_1^+|^2 L_n(u) + |\eta_2^+|^2 L_{n-1}(u), \tag{7}$$

$$G_{n,s_z,p}^- = |\eta_1^-|^2 L_{n-1}(u) + |\eta_2^-|^2 L_n(u), \tag{8}$$

where $u = C^2 l_B^2/2$, $x_0 = l_B^2 k_x$, and $L_n(u)$ are the Laguerre polynomials. The energy correction depends on the wave vector k_x through x_0. That is, the periodic potential broadens the discrete LLs into bands. Given that the polynomials $L_n(u)$ oscillate for large n, in addition to the function $\cos(Cx_0)$, one easily sees that the bandwidths (6) oscillate with the magnetic field B. For $n = 0$, the energy correction is

$$\Delta E_{0,s_z}^\pm(k_x) = V_0\cos(Cx_0)e^{-u/2}. \tag{9}$$

Note that the bandwidths (6) are different for spins up and down because of the spin-dependent coefficients $\eta_{1,2}^\pm$.

(ii) *Field modulation.* We replace the field E_z in Eq. (1) by a periodic one $E_z(y) = E_0\cos(Dy)$ with $D = 2\pi/b_0$ and b_0 is the period. The energy correction is

$$\Delta'E_{n,s_z,p}^\pm(k_x) = \langle n, s_z, p, k_x|\ell E_z(\xi)\sigma_z|n, s_z, p, k_x\rangle, \tag{10}$$

$$= \ell E_0\cos(Dx_0)e^{-u'/2}G_{n,s_z,p}'^\pm, \tag{11}$$

$$G_{n,s_z,p}'^+ = |\eta_1^+|^2 L_n(u') - |\eta_2^+|^2 L_{n-1}(u'), \tag{12}$$

$$G_{n,s_z,p}'^- = |\eta_1^-|^2 L_{n-1}(u') - |\eta_2^-|^2 L_n(u'), \tag{13}$$

where $u' = D^2 l_B^2/2$. For $n = 0$, we find

$$\Delta'E_{0,s_z}^\pm(k_x) = \pm\ell E_0\cos(Dx_0)e^{-u'/2}. \tag{14}$$

In Fig. 2, we show the broadened LLs versus the magnetic field B, for $k_x = 10^8$ m^{-1}, in the presence of a field modulation, with $b_0 = 300$ nm and $\ell E_0 = 1$ meV. We used the strength of the SOI[3] $\lambda_{so} = 3.9$ meV and the Fermi velocity $v_F = 5.42 \times 10^5$ m/s. The LLs resulting only from the potential modulation, with $a_0 = 300$ nm and $V_0 = 1$ meV, are shown in the inset. As seen, the oscillatory E_z and V lift the spin and valley degeneracy of the LLs. Each LL ($n \geq 1$) splits into four branches except for certain values of B at which $\cos(Dx_0) = 0$ and the bandwidth vanishes. That occurs at fields $B = B_c/(2m+1)$, with $B_c = 2(h/e)k_x/\pi b_0$ and m is a nonnegative integer. Notice that the $n = 0$ LL splits into *two valley branches with the same spin* as can be seen from $E_{0,s_z}^\pm = \pm\hbar\omega_c\lambda_\pm(s_z) + \Delta'E_{0,s_z}^\pm$. For positive energies, this is the down spin.

The lifting of the spin and valley degeneracy results from the fact that for $\ell E_0 = 0$ the eigenvalues (3) are spin and valley degenerate, $E_{n,s_z=\pm1,p}^+ = E_{n,s_z=\mp1,p}^- = p\hbar\omega_c(n + \bar\lambda_{so}^2)^{1/2}$, but the eigenfunctions are not since the coefficients $\eta_{1,2}^\pm$ are spin dependent, e.g., $(\eta_1^+)^2|_{s_z=\pm1} = (\eta_2^-)^2|_{s_z=\mp1} = [\mp\lambda_{so} + E_{n,s_z,p}^+]/2E_{n,s_z,p}^+$. Then, all energy corrections depend on the spin.

At very low fields B the function $\cos(Cx_0)$ in Eq. (6) fluctuates rapidly but the function $e^{-u/2}$ drastically reduces the oscillation amplitude. The same holds for the function $\cos(Dx_0)$. Once B_c is attained, the energies increase monotonically and the bandwidth ceases to oscillate. This explains the form of the $n = 0$ LL.

The dc diffusive conductivity is given by[11]

$$\sigma_{\mu\nu}^d = \frac{\beta e^2}{S}\sum_\zeta \tau_\zeta f_\zeta(1 - f_\zeta)v_{\nu\zeta}v_{\mu\zeta}, \tag{15}$$

where τ_ζ is the momentum relaxation time and $v_{\mu\zeta}$ is the diagonal matrix elements of the velocity operator. Further, $f_\zeta = [1 + \exp\beta(E_\zeta - E_F)]^{-1}$ is the Fermi-Dirac function with $\beta = 1/k_BT$ and T is the temperature. We focus here on the large-amplitude oscillations described by Eq. (12) and neglect the small-amplitude ones described by the collisional contribution.[11]
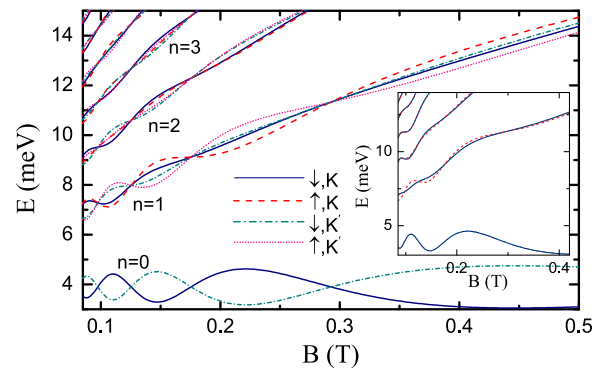

FIG. 2. Landau levels vs magnetic field B, in the presence of a field E_z modulation with $b_0 = 300$ nm and $\ell E_0 = 1$ meV. Notice that the two curves for $n = 0$ involve the same spin (down) but different valleys. The inset shows the LLs in the presence of only a potential modulation with $a_0 = 300$ nm and $V_0 = 1$ meV.

Regarding the Hall conductivity $\sigma_{\mu\nu}^{nd}$, one can cast the form used in Ref. 11 in the familiar one

$$\sigma_{\mu\nu}^{nd} = \frac{i\hbar e^2}{S} \sum_{\zeta \neq \zeta'} \frac{(f_\zeta - f_{\zeta'}) v_{\nu\zeta\zeta'} v_{\mu\zeta'\zeta}}{(E_\zeta - E_{\zeta'})^2}, \quad (16)$$

where $v_{\nu\zeta\zeta'}$ and $v_{\mu\zeta\zeta'}$ are the nondiagonal matrix elements of the velocity operator and $\mu, \nu = x, y$. The sum runs over all quantum numbers $|\zeta\rangle = |\lambda, k_x, k_y, s_z\rangle$, $|\zeta'\rangle$.

(iii) *1D periodic potential or E_z modulation.* The modulation broadens the LLs into bands, cf. Eq. (6), and this induces a group velocity, proportional to the LL bandwidth, that results in a diffusive conductivity. Then, the electron velocity in the n-th Landau band is given by

$$v_{x,n,s_z,p}^{\pm}(k_x) = -(V_0 C l_B^2/\hbar)\sin(Cx_0)e^{-u/2}G_{n,s_z,p}^{\pm}(u), \quad (17)$$

and that due to a field modulation, $v_x'^{\pm}$, by Eq. (14) with V_0, u, C, and G replaced by ℓE_0, u', D, and G', respectively. When the temperature is sufficiently low, the relaxation time can be evaluated at the Fermi energy, $\tau_\zeta \approx \tau_F$. For a weak modulation, one can neglect[12] the k_x dependence of f_ζ. The result is

$$\sigma_{xx} = \frac{e^2}{h} \frac{\beta V_0^2 \tau}{\hbar} u e^{-u} \sum_{n,s_z,p,\pm} f_\zeta(1 - f_\zeta)(G_{n,s_z,p}^{\pm})^2. \quad (18)$$

For a field modulation, we obtain Eq. (15) with V_0, u, C, and G replaced by ℓE_0, u', D, and G', respectively.

Figure 3 shows the diffusive conductivity in the presence of only a field modulation. The solid (dashed) curve is the up (down) spin contribution. The oscillations are considerably spin resolved and at certain ranges of the field B (coloured areas) a nearly 100% spin-polarized current is obtained. The two valleys make nearly the same contribution, i.e., no valley-resolved current is achieved because $|v_x'^+| = |v_x'^-|$. If only the $V(y)$ modulation is present

($|v_x^+| = |v_x^-|$), no sizable valley or spin gap is created in the oscillations, see the inset in Fig. 3. However, the oscillation amplitude is about 60 times larger than that of the field modulation because $|G_{n,s_z,p}^{\pm}| \gg |G_{n,s_z,p}'^{\pm}|$. Notice that $\sigma_{xx} \approx 0$ for $0.7\,\mathrm{T} < B < 0.8\,\mathrm{T}$.

(iv) *Potential and field modulations.* To avoid the drawbacks of a single modulation and further asses the influence of parameters on the valley and spin splittings, we can combine the two modulations. To this end, we assume that a field modulation is already present, with fixed $E_0 = 1\,\mathrm{meV}/\ell$ and $b_0 = 300\,\mathrm{nm}$, and vary the strength V_0 and period a_0 of the potential modulation. We plot the valley polarization $p_v = (\sigma_+ - \sigma_-)/(\sigma_+ + \sigma_-)$ as a function of the ratio $V_0/\ell E_0$ for different magnetic fields B in Fig. 4(a) and different periods a_0 in Fig. 4(b); the two valley conductivities σ_+ and σ_- include both spins. For low V_0, the polarization p_v is maximal, whereas for high V_0 it disappears. Moreover, p_v is maximal when the two modulations have the same period. In Fig. 4(c), we plot p_v and the spin polarization p_s, defined in a similar way, as functions of the field B for $V_0 = 0.2\,\mathrm{meV}$ and $a_0 = b_0$. As seen, the presence of both modulations leads to a sizable p_v because the total velocity differs for the two valleys; that is $|v_x'^+ + v_x^+| \neq |v_x'^- + v_x^-|$. Both p_v and p_s oscillate nearly periodically with B but their periods increase at high B, cf. Eqs. (6) and (9). In contrast to Fig. 3, the spin gap is smaller and decreases at low fields B because the LL index n near E_F is large; thus $\lambda_\pm(s_z) \ll E_{n,s_z,p}^{\pm}$ which yields $|\eta_1^{\pm}|^2 \approx |\eta_2^{\pm}|^2 \approx 1/2$.

Hall conductivity σ_{yx}. It is given by Eq. (16) and its evaluation requires the velocity operator $\hat{v} = \nabla_{\vec{\pi}}H$, which for the two valleys is given by $\hat{v}^{\pm} = v_F(\sigma_x\hat{e}_x \mp \sigma_y\hat{e}_y)$. All its matrix elements, evaluated analytically, are diagonal in k_x ($\delta_{k_x,k_x'}$). To better understand the effect of the *field E_z* modulation on σ_{yx}, we also consider a constant field E_z that leads to k_x-independent LLs. Now a periodic, weak field E_z perturbs the states $|\zeta\rangle^0$ and the new ones $|\zeta\rangle$ can be
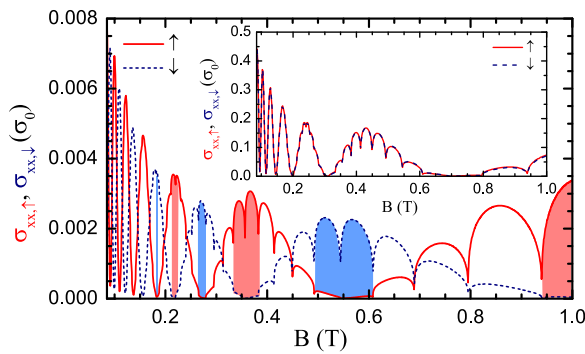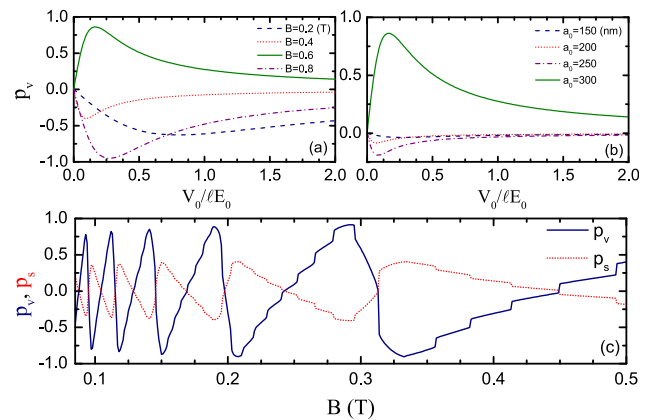

FIG. 3. Spin-up (solid curve) and spin-down (dashed curve) contributions to the diffusive conductivity, in units of $\sigma_0 = (e^2/h)\beta\tau(\ell E_0)^2/h$, versus the field B, when only the field modulation is present with $E_0 = 1\,\mathrm{meV}/\ell$, $b_0 = 300\,\mathrm{nm}$, $T = 3\,\mathrm{K}$, and $n_e = 5 \times 10^{11}\,\mathrm{cm}^{-2}$. In the coloured regions, the conductivity is nearly spin polarized and the colour is that of the dominant spin state. The inset shows results only for a potential modulation with $V_0 = 1\,\mathrm{meV}$, $a_0 = 300\,\mathrm{nm}$, and the same T and n_e. Note the increase in the oscillation amplitude.

FIG. 4. (a) Valley polarization p_v versus the ratio $V_0/\ell E_0$ for different fields B. The parameters are $E_0 = 1\,\mathrm{meV}/\ell$, $b_0 = a_0 = 300\,\mathrm{nm}$, $T = 3\,\mathrm{K}$, and $n_e = 5 \times 10^{11}\,\mathrm{cm}^{-2}$. (b) The same as in (a) but for different periods a_0 at $B = 0.6\,\mathrm{T}$. p_v is maximal for low strengths V_0 and $a_0 = b_0$. (c) Valley (solid curve) and spin (dotted curve) polarizations versus magnetic field B for $V_0 = 0.2\,\mathrm{meV}$ and $a_0 = b_0 = 300\,\mathrm{nm}$.
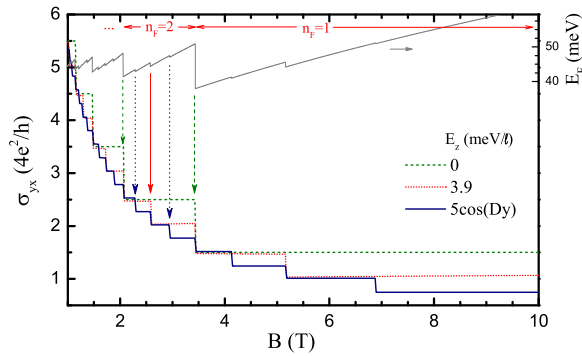
FIG. 5. (a) Hall conductivity σ_{yx} versus the field B for different electric fields E_z for *zero* temperature, $v_F = 5.42 \times 10^5$ m/s, and $N_e = 5 \times 10^{11}$ cm^{-2}. The topmost curve shows E_F versus B for a modulated E_z and the scale is on the right axis. A constant field E_z (dotted curve) doubles the number of plateaux. The intra-LL plateaux result from spin (dotted arrows) and valley (solid arrow) transitions.

approximated by first-order perturbation theory. With $(\ell E_0)_{\zeta'\zeta} =^0 \langle \zeta' | \ell E_0 \sigma_z | \zeta \rangle^0$, they read

$$|\zeta\rangle = |\zeta\rangle^0 + \sum_{\zeta' \neq \zeta} \frac{(\ell E_0)_{\zeta'\zeta}}{E_\zeta - E_{\zeta'}} |\zeta'\rangle^0. \tag{19}$$

Figure 5 shows the Hall conductivity versus the field B. The dashed, dotted, and solid curves show, respectively, the well-known plateaux for integer n ($E_z = 0$), the ones for constant field ($E_z = 3.9$ meV/ℓ), and those for a periodic field ($E_z = 5\cos(Dy)$ meV/ℓ). All of them occur precisely at those fields B at which E_F (or n_F) jumps from one LL to another (topmost curve) as indicated by the arrows for $n_F = 2$. The value $E_z = 3.9$ meV/ℓ was chosen to cancel the SOI term for spin up (down) in the K (K') valley, as in graphene which has a very weak SOI. For a constant field, all LLs split due to the spin and valley degrees of freedom and the number of sharp changes in E_F increases; the valley splitting though is very weak, hence the extra plateaux are mostly due to spin resolution. However, for a modulated field, the LL valley splitting is comparable to their spin splitting, see Fig. 2. In Fig. 5, the large plateaux (dashed curve) are replaced by a series of short plateaux and steps (solid curve) due to spin or valley transitions shown by arrows. The extra plateaux arise at fields $B = N_e \phi_0/m$; the modulation does not affect their location but only the height of the steps between them at a finite temperature.

As for the results in the presence of only a potential modulation $V(y)$: (i) they affect σ_{yx} very little, and (ii) they differ from the field modulation ones because $V(y)$ enters the Hamiltonian (1) as $V(y)I$, whereas $E_z(y)$ enters it as $E_z(y)\sigma_z$.

That is, $E_z(y)$ affects the carriers' spin and valley degrees of freedom but $V(y)$ does not.

In summary, we studied commensurability oscillations in silicene due to a weak electric field E_z and/or potential periodic modulation. A constant E_z and the strong SOI lead to spin and valley split LLs. The modulations broaden the LLs into bands and lead to a diffusive conductivity. The spin splitting due to only potential modulation is very weak but for field modulation it is relatively large, cf. Fig. 3. Also, the valley polarization p_v vanishes when only one modulation is present. These drawbacks are avoided when both modulations are present, have the same period, and the ratio of their strengths $V_0/\ell E_0$ is small, cf. Fig. 4. For $V_0/\ell E_0 \geq 1$, the spin polarization p_s and p_v disappear; both are nearly periodic in the field B, phase-shifted by π, and their periods increase with B.

We also studied the Hall conductivity σ_{yx} and showed that the field modulation creates extra narrow plateaux within the standard, integer-n LL plateaux. All of them are due to sharp changes in E_F, as it moves through the LLs, and the new ones result from the lifting of the spin and valley degeneracies and the corresponding transitions between the four ($n \geq 1$) or two ($n = 0$) sublevels. The step structure, within an integer-n LL plateau, replaces the latter by a series of narrow plateaux and steps.

[1]G. G. Guzmán-Verri and L. C. Lew Yan Voon, Phys. Rev. B **76**, 075131 (2007); S. Lebègue and O. Eriksson, Phys. Rev. B **79**, 115409 (2009).
[2]P. Vogt, P. D. Padova, C. Quaresima, J. Avila, E. Frantzeskakis, M. C. Asensio, A. Resta, B. Ealet, and G. L. Lay, Phys. Rev. Lett. **108**, 155501 (2012); A. Fleurence, R. Friedlein, T. Ozaki, H. Kawai, Y. Wang, and Y. Yamada-Takamura, Phys. Rev. Lett. **108**, 245501 (2012).
[3]C.-C. Liu, W. Feng, and Y. Yao, Phys. Rev. Lett. **107**, 076802 (2011).
[4]A. Kara, H. Enriquez, A. P. Seitsonen, L. C. Lew Yan Voon, S. Vizzini, B. Aufray, and H. Oughaddoub, Surf. Sci. **67**, 1 (2012).
[5]M. Ezawa, Phys. Rev. Lett. **109**, 055502 (2012).
[6]M. Tahir and U. Schwingenschlgl, Appl. Phys. Lett. **101**, 132412 (2012).
[7]Y. Cai, C.-P. Chuu, C. M. Wei, and M. Y. Chou, Phys. Rev. B **88**, 245408 (2013).
[8]M. Neek-Amal, A. Sadeghi, G. R. Berdiyorov, and F. M. Peeters, Appl. Phys. Lett. **103**, 261904 (2013).
[9]H. Liu, J. Gao, and J. Zhao, J. Phys. Chem. C **117**, 10353 (2013).
[10]D. Weiss, K. v. Klitzing, K. Ploog, and G. Weimann, Europhys. Lett. **8**, 179 (1989).
[11]F. M. Peeters and P. Vasilopoulos, Phys. Rev. B **46**, 4667 (1992).
[12]A. Matulis and F. M. Peeters, Phys. Rev. B **75**, 125429 (2007).
[13]R. Nasir, K. Sabeeh, and M. Tahir, Phys. Rev. B **81**, 085402 (2010).